Available online at www.sciencedirect.com
ScienceDirect
Trans. Nonferrous Met. Soc. China 25(2015) 2772−2780
Transactions of Nonferrous Metals Society of China
www.tnmsc.cn

Vapor pressure measurement of lead and lead chlorides in FeO_T−CaO−SiO_2−Al_2O_3 system

Yan-ling ZHANG[1], Eiki KASAI[2]

1. State Key Laboratory of Advanced Metallurgy, University of Science and Technology Beijing, Beijing 100083, China;
2. Graduate School of Environmental Studies, Tohoku University, 6-6-20 Aramakiazaaoba, Aoba-ku, Sendai Miyagi 980-8579, Japan

Received 22 September 2014; accepted 10 March 2015

Abstract: Vapor pressure of lead and lead chlorides from FeO_T−CaO−SiO_2−Al_2O_3 slag system was measured by using Knudsen effusion method. The results suggest that the vapor pressures of lead and lead chlorides increase with increasing temperature. For the slag systems without chlorine, the logarithm of vapor pressure (ln$p$) shows highly linear dependency on the reciprocal of temperature ($1/T$), and higher vapor pressure is observed in the condition where more metallic lead vapor is formed. In this case, the vapor pressure of lead increases with increasing slag basicity (w(CaO)/w(SiO_2)), increasing FeO content and w(Fe^{2+})/w(Fe^{3+}) ratio. For the case of slag system with chlorine addition, the total pressures of $PbCl_2$ and PbCl increase with decreasing basicity and FeO content of slag.

Key words: vapor pressure; Knudsen effusion method; metallic Pb; lead chlorides; smelting process

1 Introduction

Smelting process has been accepted as a practical method to treat fly ashes and dust containing heavy metals. During this process, volatile metal elements such as lead and zinc can be separated from the residue by evaporation [1,2], while the oxide residue (sometimes referred to as slag) could be inert to the environment. Since toxic organic compounds in wastes are completely destroyed due to a long residence time at high temperatures, permanently safe slag products can be achieved if the heavy metals are appropriately removed.

In order to effectively control the removal process of the heavy metals from fly ashes, much basic knowledge is very important such as vapor pressures, activities, and interactions in molten materials of these metals. Previous experimental research has been performed on the vaporization behaviors and the related kinetic information of heavy metals under incineration and thermal treatment conditions [3−5], along with thermodynamic predictions for the formation of vapor species [6−8]. However, the data available regarding vapor pressures, activities, and interactions with matrix are limited.

Several methods have been applied to determining saturated vapor pressures. Knudsen effusion method is one of the most accurate techniques for measurement of much lower vapor pressure [9,10]. This method has long been employed for measurements of organic compounds [11−13]. ZHANG et al [14] have ever used this method to obtain the vapor pressure of zinc and zinc chlorides from complex system, while the other applications on measurements of metal chlorides are rarely reported.

According to the typical compositions of waste incineration ashes [15,16], FeO_T−CaO−SiO_2−Al_2O_3-based slag system tends to be formed during smelting treatment. In this work, the vapor pressure of lead from FeO_T−CaO−SiO_2−Al_2O_3 system with and without chlorine was measured under varying conditions of the parameters such as temperature and slag compositions.

2 Experimental

2.1 Sample preparation

Three kinds of FeO−CaO−SiO_2−Al_2O_3 slag located

Foundation item: Project supported by the Japan Oil, Gas and Metals National Corporation (JOGMEC); Project (51474021) supported by the National Natural Science Foundation of China
Corresponding author: Yan-ling ZHANG; Tel: +86-10-82375842; Fax: +86-10-82375828; Email: zhangyanling@metall.ustb.edu.cn
DOI: 10.1016/S1003-6326(15)63902-4

at the edges of the liquid-stable region at low temperature of 1150 °C were selected: F-slag with the highest FeO content, C-slag with the highest CaO content, and S-slag with the highest SiO_2 content. The chemical compositions of the slags are shown in FeO−CaO−SiO_2−5%Al_2O_3 system (Fig. 1), which were well mixed and kept in an aluminum crucible. The crucible was then placed in an electric furnace controlled and heated to 1210 °C for 2 h in Ar atmosphere. Finally, the slag was water cooled. The chemical compositions of produced slags are listed in Table 1. The pre-melt slags are ground into powder and then mixed with chemical reagents of PbO, whose content is fixed at 10% in the chlorine-free slag, while that is kept at 5% and $CaCl_2$ is then added by controlling the molar ratio of $n(CaCl_2)$: n(PbO) at 1:1 in the chlorine slag.

2.2 Experimental apparatus and procedures

A schematic diagram of the apparatus is shown in Fig. 2. A cylindrical cell whose schematic structure was introduced in Ref. [17] made of pure platinum with equal height and diameter (D=H=10 mm) was used. The balance yields a minimum accuracy of 0.01 mg. A high vacuum condition (lower than 10^{-2} Pa) was maintained by a turbo molecular pump and a rotary pump. The temperature of the sample was controlled by a regulated electric furnace. The mass loss of the sample was continuously recorded by a data acquisition system.

Since the diameter of orifice is very small, an apparent equilibrium condition can be maintained inside the cell. The saturated vapor pressure of the sample can be obtained by Eq. (1)[17].

$$P_e = \frac{1}{K_C A_0} \cdot \frac{\Delta m}{t} \cdot \sqrt{\frac{2\pi RT}{M}} \quad (1)$$

where P_e represents the saturated vapor pressure of the sample, Pa; A_0 is the area of the orifice, m^2; M is the molecular mass of the effusing vapor, kg/mol; t is the experimentation time, s; Δm is the mass loss of the sample, kg; T is temperature, K, and R is the mole gas constant, 8.314 J/(mol·K); K_C is a coefficient reflecting

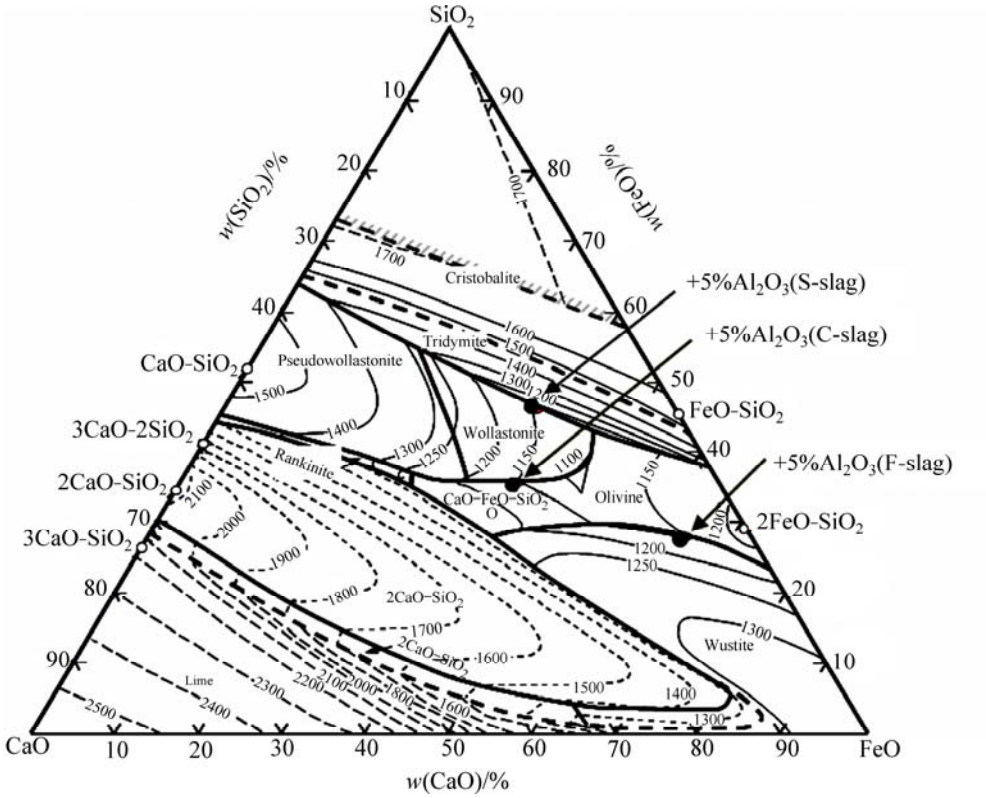

Fig. 1 Phase diagram of FeO−CaO−SiO_2 system and experimental slag condition

Table 1 Chemical compositions of produced slag

Slag sample	w(CaO)/%	w(SiO_2)/%	w(FeO)/%	w(Al_2O_3)/%	w(Fe_2O_3)/%	$w(Fe^{2+})/w(Fe^{3+})$	Basicity
C-slag	21.27	31.91	13.96	4.66	28.2	0.55	0.67
S-slag	17.87	44.19	17.80	4.95	15.19	1.30	0.40
F-slag	6.96	24.35	54.41	4.58	9.70	6.20	0.29

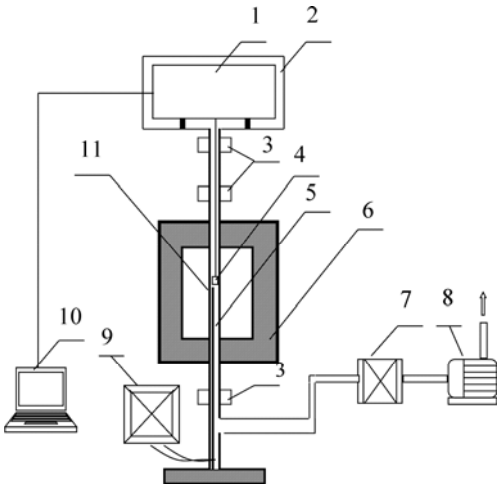

Fig. 2 Schematic drawing of apparatus for Knudsen effusion measurement: 1—Balance; 2—High vacuum room; 3—Water cooling; 4—Knudsen cell; 5—Thermocouple; 6—Electric furnace; 7—Turbo molecular pump; 8—Rotary pump; 9—Temperature controller; 10—Data system; 11—Reaction tube

the transmission probability of gas molecules throughout the orifice, since some molecules entering the orifice would strike the wall of the orifice and return to the cell rather than escape out of the cell. For a typical orifice of cylindrical shape, K_C can be evaluated by the orifice length (thickness of the cell) L and its radius r [10]:

$$K_C = \frac{1+\frac{0.4L}{r}}{1+\frac{0.95L}{r}+0.15(\frac{L}{r})^2} \quad (2)$$

Equation (1) holds under the conditions that there are no collisions between the molecules either in the cell or near the orifice and the escaped molecules do not disturb the equilibrium between the vapor and the condensed phases. These conditions are established when the mean free path of the molecule λ, which is determined by the vapor pressure and temperature, is larger than the diameter of the orifice d and when the surface area of the condensed phase A_S is sufficiently larger than the orifice area A_0. Generally, it was recommended [9,10] that Eq. (1) is accurate when λ/d=1−10 and A_0/A_S<0.01.

3 Results and discussion

3.1 Case for slag system without chlorine addition

3.1.1 Vapor species prediction based on thermodynamic calculation

The possible vapor species of lead generated in the present slag system was predicted by using thermodynamic code FactSage based on minimizing Gibbs free energy minimization, together with its solution database. The considered reactants are FeO, Fe_2O_3, CaO, SiO_2, Al_2O_3, and PbO with the same compositions as that of experimental sample. The vapor species of Pb and their distribution in gas phase from different slag systems as functions of temperature are shown in Fig. 3(a), and the effects of basicity, FeO content in slag, and initial PbO content are shown in Figs. 3(b), (c), and (d), respectively. In F-slag, mainly metallic Pb vapor is formed in the temperature range from 1100 K to 1700 K, and the vaporization of PbO could be neglected. The related reaction can be expressed as Eq. (3), where c represents a condense state:

$$2FeO(c)+PbO(c)=Pb(g)+Fe_2O_3(c) \quad (3)$$

The standard Gibbs free energy change of the Reaction (3) is positive in the experimental temperature range between 1173 and 1573 K. While, due to the relatively low partial pressure of metallic Pb, it could be negative and the reaction proceeds to the right side under the actual condition. However, in the condition of C- and S-slag systems, the mixture of metallic Pb and PbO vaporizes into gas phase, and the ratio of PbO in vapor greatly increases with increasing temperature (Fig. 3(a)). The reason behind this could be explained by the lower $w(Fe^{2+})/w(Fe^{3+})$ ratio in C- and S-slag systems, which tends to prohibit Eq. (3) to move to the right side. Under the same temperature, the ratio of metallic Pb in gas phase increases in the order of C-slag<S-slag<F-slag, as illustrated in Fig. 3(a), which consists well with the increasing order of $w(Fe^{2+})/w(Fe^{3+})$ ratio in these slag samples ($w(Fe^{2+})/w(Fe^{3+})$ ratios in C-slag, S-slag, and F-slag are 0.55, 1.30, and 6.20, respectively, shown in Table 1). On the other hand, in this temperature range, the high volatile property of PbO makes it directly vaporized into gas phase. Further, the previous research [18] revealed that compared with ZnO, PbO tends to give less affinity with slag compositions such as SiO_2 and Al_2O_3. This could be another reason causing direct vaporization of PbO into gas phase.

Further, Fig. 3(b) suggested that in the case of $w(Fe^{2+})/w(Fe^{3+})$=6.2 more than 96% of lead exited in the form of metallic Pb in vapor under 1383 K, and the effect of slag basicity could be neglected. Figure 3(c) shows the distribution of lead in gas phase as functions of FeO content in the samples based on S-slag condition, whose basicity is set as 0.4, Al_2O_3 content is 4.95%, total content sum of CaO, SiO_2, and Al_2O_3 is kept unchanged and the same with that of S-slag. Accordingly, the total content sum of FeO and Fe_2O_3 is also the same with that of S-slag, which means that the increase in FeO content causes a decrease in Fe_2O_3 content and an increase in $w(Fe^{2+})/w(Fe^{3+})$ ratio. As shown, FeO content and $w(Fe^{2+})/w(Fe^{3+})$ ratio in slag give considerable influence

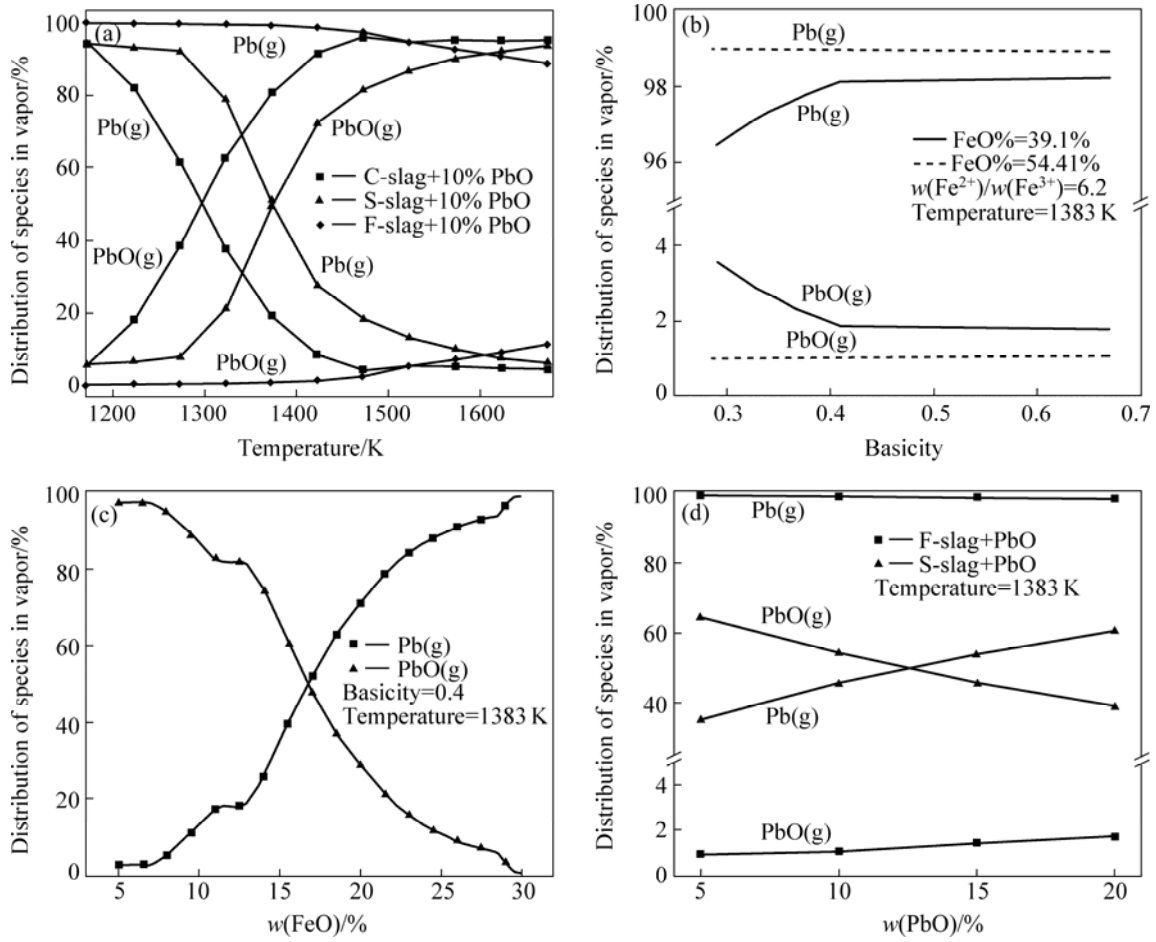

Fig. 3 Thermodynamic predictions on distribution of lead species in vapor from slag without chlorine

on the vapor species of lead under 1383 K. With increasing FeO content and $w(Fe^{2+})/w(Fe^{3+})$ ratio, the ratio of metallic Pb in vapor greatly increases while that of PbO decreases. Additionally, in a slag with FeO content and $w(Fe^{2+})/w(Fe^{3+})$ ratio as high as that of F-slag, the initial PbO content gives extremely limited effect on vapor species of lead (as shown in Fig. 3(d)), and metallic Pb tends to be only species in vapor; while in S-slag, both of metallic Pb and PbO vapor simultaneously vaporize into gas, and the ratio of metallic Pb tends to increase with an increase in the initial PbO content (Fig. 3(d)).

Since an equilibrium state tends to be approached in Kundsen cell, the vapor species under different situations could be estimated based on the above calculation. If the ratio of PbO in vapor is small enough to be neglected, the vapor pressure of metallic Pb can be obtained by Eq. (1). In other cases, both of metallic Pb and PbO contribute to the total mass loss of the sample. For the sake of simplicity, their total vapor pressure, expressed as p_{Pb+PbO} in this wrok, was estimated by Eq. (1), where M was set as the average value of molecular mass of PbO and metallic Pb.

3.1.2 Effect of temperature on vapor pressure of metallic Pb and PbO

As known, Knudsen effusion method is reasonably applicable in the case of lower vapor pressure. Furthermore, a certain mass loss is necessary to assure the accuracy of the mass measurement. Accordingly, the measurement temperature range (1173−1573 K) was determined considering these conditions. Figure 4 shows the temperature dependency of the vapor pressure of lead from different slag samples of 90%slag+10%PbO. Based on the thermodynamic prediction in Fig. 3, metallic Pb tends to be the only vapor specie in F-slag condition under measurement temperature (1233−1383 K). The data in Fig. 4 suggest that the vapor pressure of metallic Pb increases significantly with increasing temperature, and a good linear relationship between the logarithmic of vapor pressure of metallic Pb ($\ln p_{pb}$) and the reciprocal of temperature ($1/T$) is observed for 90% F-slag + 10% PbO at 1233−1383 K:

$$\ln p_{Pb}=-5.1/T+9.2 \quad (4)$$

As introduced above, the Knudsen measurement has been carried out under an equilibrium condition, hence the corresponding Gibbs free energy should be zero.

Therefore, Eq. (5) can be gotten:

$$\ln\frac{(p_{Pb}/101325)\cdot a_{Fe_2O_3}}{a_{FeO}^2\cdot a_{PbO}}=-\frac{\Delta H_3^{\Theta}}{RT}+\frac{\Delta S_3^{\Theta}}{R} \quad (5)$$

where ΔH_3^{Θ} and ΔS_3^{Θ} represent the standard enthalpy and standard entropy of Eq. (3), respectively; p_{pb} (Pa) is the vapor pressure of metallic Pb; $a_{Fe_2O_3}$, a_{FeO}, and a_{PbO} represent the activities of Fe_2O_3, FeO, and PbO in slag, respectively. According to the measurement results, the logarithm of metallic Pb pressure ($\ln P_{Pb}$) is a linear function of the reciprocal of temperature ($1/T$). This implies that the ratio of $\frac{a_{Fe_2O_3}}{a_{FeO}^2 a_{PbO}}$ is kept at a constant value under these experimental situations. Based on the measurement results on the vapor pressure of metallic Zn from similar slag samples [14], the logarithm of metallic Zn pressure ($\ln p_{Zn}$) is a highly non-linear function of $1/T$, which was explained by the authors that the activities of Fe_2O_3 and FeO change in the temperature range of Reaction (6). These indicate that even through zinc and lead have similar volatile properties, their compounds give different interacting mechanisms with slag matrix.

$$2FeO(c)+ZnO(c)=Zn(g)+Fe_2O_3(c) \quad (6)$$

For S- and C-slag samples (90%S-slag+10%PbO and 90%C-slag+10%PbO), metallic Pb and PbO coexisted in vapor phase (Fig. 3(a)) under 1283−1533 K. The total vapor pressure of metallic Pb and PbO increases with the increase in temperature. Further, it is observed that the logarithmic of vapor pressure of metallic Pb and PbO ($\ln p_{Pb+PbO}$) linearly depends on the reciprocal of temperature ($1/T$) in both of 90%S-slag+10%PbO and 90%C-slag + 10%PbO samples at 1283−1533 K, respectively:

$$\ln p_{Pb+PbO}=11.2/T+11.0 \quad (7)$$

$$\ln p_{Pb+PhO}=15.1/T+13.7 \quad (8)$$

In addition, Fig. 4 suggests that the vapor pressure of metallic Pb from F-slag sample is much higher than the total pressure of metallic Pb and PbO from C- and S-slag samples, while the difference between these two cases decreases with the increase of temperature. It clearly shows that a higher vapor pressure tends to be obtained in a matrix where the formation of metallic Pb is favored; while for a sample having lower FeO content and lower $w(Fe^{2+})/w(Fe^{3+})$ ratio (the formation of metallic Pb is prohibited), an increase in temperature is more effective to promote the evaporation of lead.

3.1.3 Effect of initial PbO content

Thermodynamic predictions in Fig. 2(d) suggest that in initial PbO content range from 5% to 20%, metallic Pb tends to be the only species in vapor from F-slag, while both of metallic Pb and PbO vaporize into gas phase from S-slag. Figure 5 shows the vapor pressure of lead from these two samples as a function of the initial PbO content. As can be seen, the vapor pressure increases with an increase of the initial PbO content. There are good linear relationships between the logarithmic of vapor pressure and the initial content of PbO in both of F- and S-slag samples, expressed as follows respectively:

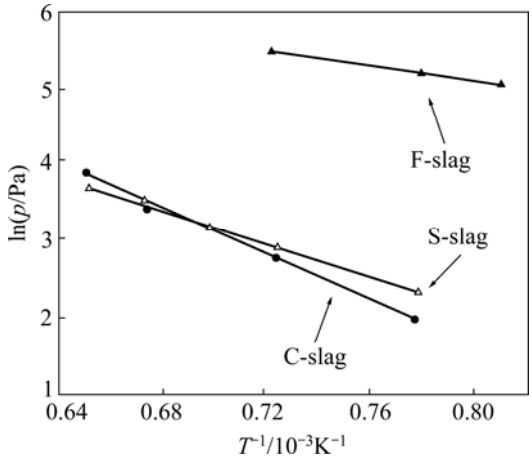

Fig. 4 Temperature dependency of vapor pressure of lead from different slag samples

$$\ln p_{Pb}=0.2w(PbO)+3.07 \quad (9)$$

$$\ln p_{Pb+PbO}=0.09w(PbO)+1.82 \quad (10)$$

where w(PbO) represents the initial mass fraction of PbO. For F-slag sample, according to the Eq. (3), the equilibrium constant K_{eq} of forming metallic Pb vapor can be expressed as follows:

$$K_{eq}=\frac{p_{Pb}\cdot a_{Fe_2O_3}}{a_{FeO}^2 a_{PbO}} \quad (11)$$

where p_{Pb} can be expressed as $p_{Pb}/101325$. Accordingly, p_{Pb} should be linearly dependent on w(PbO), when the activity coefficient of PbO is kept constant in the range of PbO content. Figure 5 shows linear relationships between $\ln p_{Pb}$ and w(PbO), which suggests a non-linear dependency of p_{Pb} on w(PbO). A possible reason for the non-linear relationships for w(PbO) in Eq. (9) could be attributed to the concentration dependent of the activity coefficient of PbO. Similar non-linear tendency was observed between the vapor pressure of metallic Zn and initial ZnO content in slag sample [14]. That also indicated that the activity coefficient of ZnO varied under varying concentrations of ZnO in slag system.

3.1.4 Effect of slag compositions on vapor pressure of lead

Figure 6 shows the measured vapor pressures of lead as a function of slag basicity (w(CaO)/w(SiO_2),

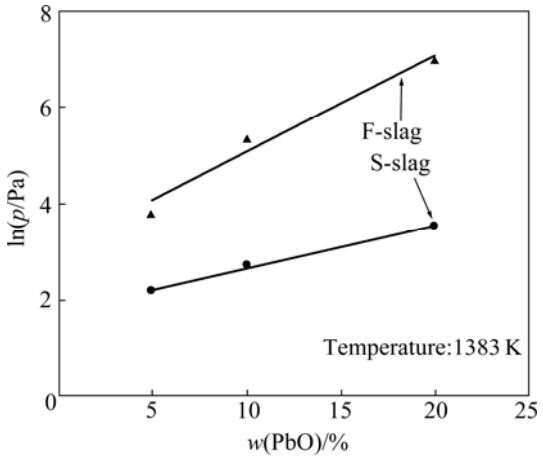

Fig. 5 Effect of initial PbO content on vapor pressure of metallic Pb

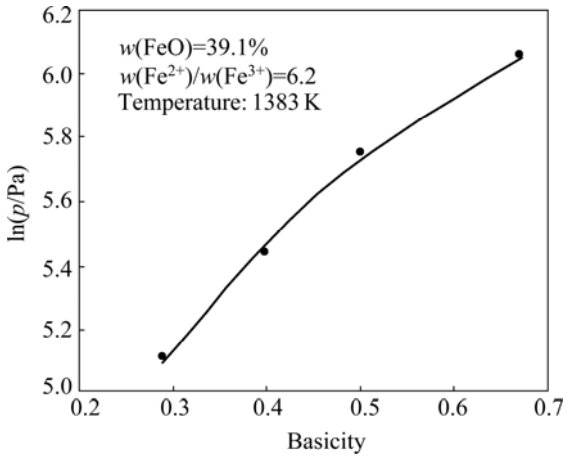

Fig. 6 Effect of slag basicity on vapor pressure of metallic Pb

where the FeO content and $w(Fe^{2+})/w(Fe^{3+})$ ratio were kept at 39.1% and 6.2, respectively. Based on the thermodynamic predictions in Fig. 3(b), in this case, metallic Pb is the major vapor species and the mass of PbO in gas phase tends to be neglected. The data in Fig. 6 suggest that the vapor pressure of metallic Pb increases with the increase in the slag basicity, which could be explained by the fact that the increase in basicity increases the PbO activity because of a stronger affinity between CaO and other slag components such as SiO_2 and Fe_2O_3. The vapor pressure of metallic Zn showed similar dependency on basicity of slag [14]. TASKINEN et al [19] and MATSUZAKI et al [20] measured the activity of PbO in PbO−CaO−SiO_2 and CaO−SiO_2−Al_2O_3 system, respectively. Both of their results suggested that the activity coefficient of PbO increases with increasing slag basicity, which reasonably agrees well with these experimental results.

The vapor pressures of lead as a function of FeO content in the slag with same basicity and different $w(Fe^{2+})/w(Fe^{3+})$ ratios are shown in Fig. 7. As seen, the vapor pressure of lead increases with increasing FeO content. A much larger increase happens when raising (w(FeO) and $w(Fe^{2+})/w(Fe^{3+})$) from (17.8%, 1.3) to (29.8%, 6.2). After that, the growth of vapor pressure slows down. Thermodynamic predictions in Figs. 3(b) and (c) show that when keeping $w(Fe^{2+})/w(Fe^{3+})$=6.2, metallic Pb tends to the only vapor species; while in the case of S-slag condition (w(FeO)=17.8%, $w(Fe^{2+})/w(Fe^{3+})$=1.3), both of metallic Pb and PbO coexisted in vapor gas. The data in Fig. 7 indicate that: 1) higher vapor pressure is obtained in the condition where more metallic Pb is formed rather than PbO vapor; 2) in the case of $w(Fe^{2+})/w(Fe^{3+})$ ratio at a level as high as 6.2, the attribution of increasing FeO content to enhance the vaporization of lead is relatively limited.

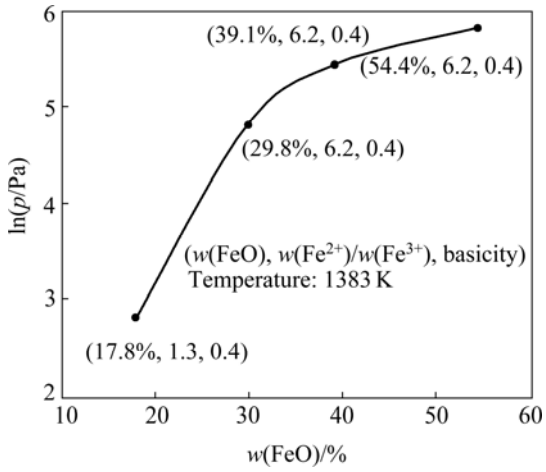

Fig. 7 Effect of FeO content in slag on vapor pressure of metallic Pb

3.2 Case for slag system with chlorine addition

3.2.1 Vapor species prediction based on thermodynamic calculation

Major vapor species formed from the sample, 95%F-slag+5%PbO+$CaCl_2$(n(PbO):n($CaCl_2$)=1:1), were predicted by the calculation using FactSage based on the principle of Gibbs free energy minimization. The considered reactants are FeO, Fe_2O_3, CaO, SiO_2, Al_2O_3, PbO, and $CaCl_2$ with the same compositions as that of experimental sample. The thermodynamic solution database was utilized, and the possible products were identified (gas phase, pure liquid, pure solids, slag, and spinel), together with the atmosphere (pure Ar), temperature range (673−2073 K) and total pressure (1.01×10^5 Pa). The vapor species of Pb and their distribution in gas phase as functions of temperature are shown in Fig. 8. Four types of vapor species, metallic Pb, $PbCl_2$, PbCl, and PbO, are dominant in the present system at temperatures between 773 and 2073 K. The proposed chemical forming reactions of metallic Pb, $PbCl_2$, and PbCl are expressed by Eqs. (3), (12) and (13),

respectively. As seen, when temperature is higher than 1473 K, PbO would directly vaporized into gas phase due to its higher vapor pressure.

$$PbO+CaCl_2=PbCl_2+CaO \quad (12)$$

$$2FeO+2PbO+CaCl_2=Fe_2O_3+2PbCl+CaO \quad (13)$$

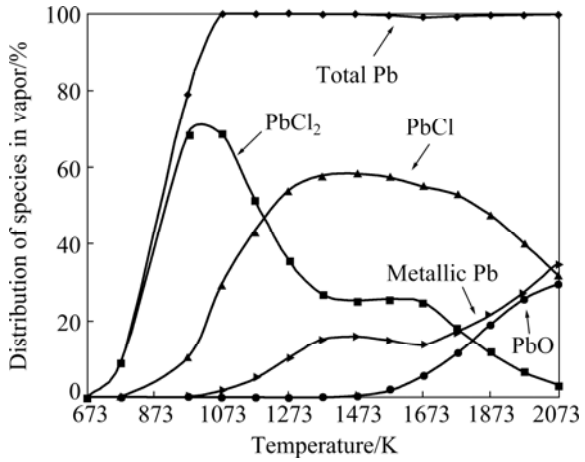

Fig. 8 Vapor species distribution of Pb as functions of temperature from F-slag

Figure 8 suggests that with increasing temperature to be higher than 973 K, the formation of $PbCl_2$ tends to be prohibited, while metallic Pb and PbCl are major vapor species under higher temperatures. As seen in Fig. 8, $PbCl_2$ and PbCl are the main species of the vapor in the measuring temperature range from 773 to 853 K, while the ratios of metallic Pb could be neglected. A considerably small amount of the metallic Pb vapor is estimated to be produced in C- and S-slag samples due to their lower reduction atmosphere. Therefore, under the present experimental conditions, it is assumed that $PbCl_2$ and PbCl are the vapor species and contribute to the total mass loss of the sample. For the sake of simplicity, their total vapor pressure, expressed as p_{PbCl_x} in this work, was estimated by using Eq. (1), where M was set as the average value of molecular mass of $PbCl_2$ and PbCl.

3.2.2 Temperature dependency of vapor pressure of lead chlorides

Temperature dependency of p_{PbCl_x} for the sample 95%slag+5%PbO+$CaCl_2$ ($n(CaCl_2)$:n(PbO)=1:1) is shown in Fig. 9. The total vapor pressure of $PbCl_2$ and PbCl increases with increasing temperature. Non-linear relationships are observed between $\ln p_{PbCl_x}$ and $1/T$. Thermodynamic predictions shown in Fig. 8 reveal that higher temperature can greatly enhance the distribution of total lead vapor into gas phase under the experimental temperature of 773−853 K. However, two kinds of lead chlorides species (PbCl and $PbCl_2$) are formed and their ratios in gas phase differ over different temperatures. With increasing temperature, the formation of PbCl vapor tends to be promoted, while that of $PbCl_2$ is prohibited. This tendency was validated by the previous experimental results [21] on vaporization behaviors of Pb from chlorine-bearing slag, where the mole ratio of Cl to Pb in gas phase decreases with the increase in temperature.

3.2.3 Effect of slag compositions

Figure 10 shows p_{PbCl_x} as a function of FeO content in slag for the sample 95%slag+5%PbO+$CaCl_2$ ($n(CaCl_2)$:n(PbO)=1:1) at 833 K. It indicates that the vapor pressure of $PbCl_2$ and PbCl decreases with the increase of FeO content. The reason behind this could be explained by that with the increase of FeO content, Eq. (13) would be promoted to move to right side enhancing the formation of PbCl species. As known, the vapor pressure of PbCl is much lower than that of $PbCl_2$, therefore, a larger PbCl ratio and the subsequent smaller $PbCl_2$ ratio in gas phase resulted in a decreased p_{PbCl_x}.

Figure 11 shows the effect of basicity on the vapor pressure of $PbCl_2$ and PbCl obtained for the sample 95% slag+5%PbO+$CaCl_2$($n(CaCl_2)$:n(PbO)=1:1) at a constant FeO content of 39%. Unlike the case without chlorine

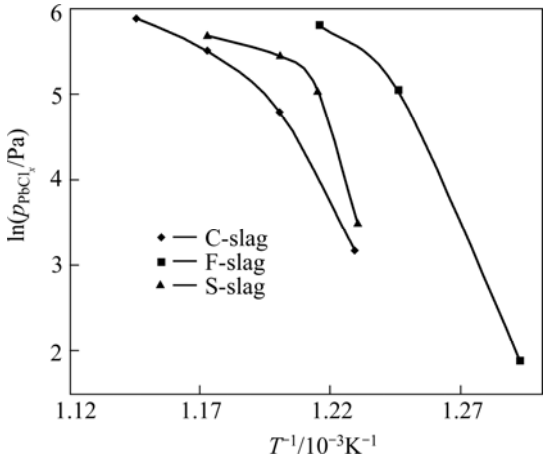

Fig. 9 Temperature dependency of lead chlorides

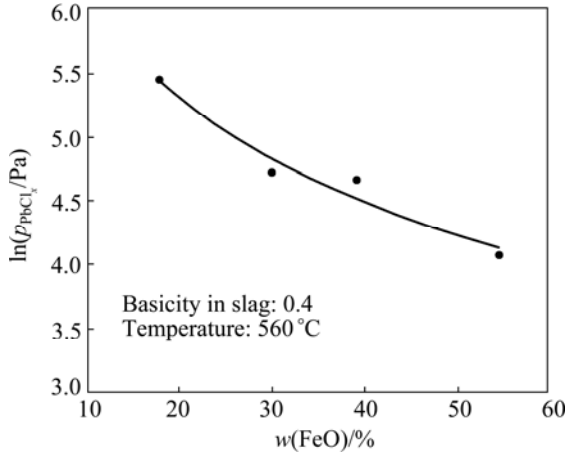

Fig. 10 Effects of FeO content in slag on vapor pressure of $PbCl_2$ and PbCl

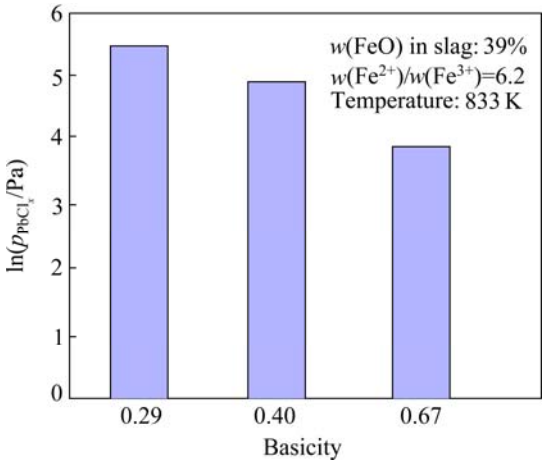

Fig. 11 Effect of basicity on vapor pressure of lead chlorides

addition, p_{PbCl_x} decreases with increasing slag basicity, which is similar with the dependency of $ZnCl_2$ pressure on slag basicity [14]. One of the explanations could be due to that the resulting large activity of CaO tends to prevent the Reaction (12) and prohibit the formation of $PbCl_2$. The previous researches [22,23] have reported that the Cl activity in slag decreases with increasing basicity of the slag system of $CaO-SiO_2-FeO/Al_2O_3$, which leads to the suppression of metal chlorides formation such as $PbCl_2$ and $ZnCl_2$. On the other hand, with increasing basicity, the activity of Fe_2O_3 in slag decreases, which is caused by strong affinity between CaO and Fe_2O_3. Consequently, Eq. (13) is enhanced to move to the right side and the formation of PbCl vapor is promoted. Similarly, p_{PbCl_x} decreases due to higher PbCl ratio. Experimental results [21] on vaporization behaviors of Pb from slag indicated that with similar content of FeO in slag, the mole ratio of Cl to Pb in gas decreased under higher slag basicity. This suggests that more PbCl and less $PbCl_2$ are generated with increasing basicity of slag. Further, the data [21] showed that volatile ratio of Pb into gas phase decreased with increasing basicity of chlorine-bearing slag. That could be explained by that the total pressure of lead chlorides decreases, leading to lower driving force of evaporation, which reasonably agrees well with this research.

4 Conclusions

1) The vapor pressures of lead and lead chlorides increase with increasing temperature. For the slag systems without chlorine addition, the logarithm of vapor pressure shows highly linear dependency on the reciprocal of temperature.

2) For slag system without chlorine, higher vapor pressure is observed in the condition where more metallic Pb vapor is formed. And the vapor pressure of lead increases with increasing slag basicity, increasing FeO content and $w(Fe^{2+})/w(Fe^{3+})$ ratio.

3) The total pressure of $PbCl_2$ and PbCl increases with decreasing basicity and FeO content of slag.

References

[1] ZHANG Yan-ling, FU Zhong-hua, LI Shi-qi, WANG Yu-gang, FU Xian-bin. Vapor pressure measurements of zinc and lead chlorides in complex system [J]. The Chinese Journal of Nonferrous Metals, 2011, 21(2): 450−458. (in Chinese)

[2] YU Jie, SUN Lu-shi, XIANG Jun, HU Song, SU Sheng, QIU Jian-rong. Vaporization of heavy metals during thermal treatment of model solid waste in a fluidized bed incinerator [J]. Chemosphere, 2012, 86(11): 1122−1126.

[3] YU Jie, SUN Lu-shi, XIANG Jun, HU Song, SU Sheng. Kinetic vaporization of heavy metals during fluidized bed thermal treatment of municipal solid waste [J]. Waste Management, 2012, 33(2): 340−346.

[4] FALCOZ Q, GAUTHIER D, ABANADES S, PATISSON F, FLAMANT G. A general kinetic law for heavy metal vaporization during municipal solid waste incineration [J]. Process Saf Environ Prot, 2010, 88(2): 125−130.

[5] LUAN Jing-de, LI Run-dong, ZHANG Zhi-hui, LI Yan-long, ZHAO Yun. Influence of chlorine, sulfur and phosphorus on the volatilization behavior of heavy metals during sewage sludge thermal treatment [J]. Waste Management and Research, 2013, 31(10): 1012−1018.

[6] ZHANG Yan-guo, LI Qing-hai, JIA Jin-yan, MENG Ai-hong. Thermodynamic analysis on heavy metals partitioning impacted by moisture during the MSW incineration [J]. Waste Management, 2012, 32(12): 2278−2286.

[7] LIU Jing-yong, SUN Shui-yu. Thermodynamic equilibrium analysis of heavy metals speciation transformation and distribution during sewage sludge incineration [J]. The Chinese Journal of Nonferrous Metals, 2010, 20(8): 1645−1655. (in Chinese)

[8] YAN Jian-hua, ZHU Hong-mei, JIANG Xu-guang, CHI Yong, CEN Ke-fa. Speciation of Cd/Cu/Pb/Zn during medical waste incineration [J]. Journal o f Zhejiang University (Engineering Science), 2008, 42(10): 1812−1816. (in Chinese)

[9] ARLSON K D. The characterization of high-temperature vapors [M]. New York: John Wiley and Sons, Inc, 1967: 115−129.

[10] CATER E D. Physicochemical measurements in metals research [M]. New York: John Willey and Sons, Inc, 1970: 22−90.

[11] FONSECA J M S, GUSHTEROV N, DOHRN R. Vapour pressures of selected organic compounds down to 1 mPa, using mass-loss Knudsen effusion method [J]. The Journal of Chemical Thermodynamics, 2014, 73: 148−155.

[12] FU Jin-xia, SUUBERG E M, Solid vapor pressure for five heavy PAHs via the Knudsen effusion method [J]. The Journal of Chemical Thermodynamics, 2013, 43(11): 1660−1665.

[13] NAKAJOH K, SHIBATA E, TODOROKI T, OHARA A, NISHIZAWA K, NAKAMURA T. Measurement of temperature dependence for the vapor pressures of twenty-six polychlorinated biphenyl congeners in commercial Kanechlor mixtures by the Knudsen effusion method [J]. Environ Toxicol Chem, 2006, 25(2): 327−336.

[14] ZHANG Yan-ling, SHIBATA E, KASAI E, NAKAMURA T. Vapor pressure of zinc and zinc chloride in the $FetO-CaO-SiO_2-Al_2O_3$ slag system [J]. Mater Trans, 2006, 47(5): 1341–1346.

[15] YOSHIIE R, NISHIMURA M, MORITOMI H. Influence of ash composition on heavy metal emissions in ash melting process [J]. Fuel, 2002, 81(10): 1335−1340.

[16] WU Kai, SHI Hui-sheng, SCHUTTER G D, GUO Xiao-lu, YE

Guang. Preparation of alinite cement from municipal solid waste incineration fly ash [J]. Cement & Concrete Composites, 2012, 34(3): 322−327.

[17] ZHANG Yan-ling, SHIBATA E, KASAI E, NAKAMURA T. Vapor pressure measurements for metal chloride systems by the Knudsen effusion method [J]. Mater Trans, 2005, 46(6): 1348−1353.

[18] ZHANG Yan-ling, FU Zhong-hua, WANG Yu-gang, LI Shi-qi. Vapor pressure measurements of zinc and lead chlorides from slag system [C]// Proceedings of AISTech. Pittsburgh: AISTech, 2010: 255−270.

[19] TASKINEN P., TASKINEN A, HOLAPPA L E. Solution thermodynamics of PbO−CaO−SiO_2 melt [J]. Can Metall Q, 1982, 21(2): 163−169.

[20] MATSUZAKI K, ISHIKAWA T, TSUKADA T, ITO K. Distribution equilibria of Pb and Cu between CaO−SiO_2−Al_2O_3 melts and liquid copper [J]. Metall Mater Trans B, 2000, 31(6): 1261−1266.

[21] ZHANG Yan-ling, ZHANG Rui, KASAI E, LI Shi-qi. Vaporization behavior of lead from the FeO−CaO−SiO_2−Al_2O_3 slag system [J]. J Uni Sci Tech Beijing, 2008, 15(6): 671−677. (in Chinese)

[22] MIWA M, MORITA K, Chloride capacities of CaO−SiO_2−Al_2O_3(−FeO, MgO, MnO) slags and their application in the incineration processes [J]. ISIJ Int, 2002, 42(10): 1065−1070.

[23] HIROSUMI T, MORITA K. Solubility of chlorine in aluminosilicate slag systems [J]. ISIJ Int, 2000, 40(10): 943−948.

FeO_T−CaO−SiO_2−Al_2O_3渣系中铅及其氯化物蒸汽压测定

张延玲[1]，Eiki KASAI[2]

1. 北京科技大学 钢铁冶金新技术国家重点实验室，北京 100083；
2. Graduate School of Environmental Studies, Tohoku University, 6-6-20 Aramakiazaaoba, Aoba-ku, Sendai Miyagi 980-8579, Japan

摘　要：利用 Knudsen 喷射法测试 FeO_T−CaO−SiO_2−Al_2O_3 渣系中铅及其氯化物的蒸汽压。结果显示该复杂体系中铅及其氯化物的蒸汽压随温度升高而升高。对于不含氯元素的渣系，铅的挥发气体种类为 PbO 和金属 Pb。二者蒸汽压的对数(ln$p$)与温度的倒数(1/T)之间呈良好的线性关系。金属 Pb 蒸汽形成比例越高，总的蒸汽压越高。铅的蒸汽压随 FeO_T−CaO−SiO_2−Al_2O_3 渣系碱度的升高、随 FeO 含量及 $w(Fe^{2+})/w(Fe^{3+})$比例的升高而升高。对于含有 Cl 元素的渣系，铅的挥发气体种类为 $PbCl_2$ 和 PbCl，二者总的蒸汽压随渣碱度及 FeO 含量的降低而升高。

关键词：蒸汽压；Knudsen 喷射法；金属 Pb；铅氯化物；熔融处理工艺

(Edited by Yun-bin HE)